J Nanopart Res (2011) 13:3377–3391
DOI 10.1007/s11051-011-0256-8

RESEARCH PAPER

Nanosized aerosols from consumer sprays: experimental analysis and exposure modeling for four commercial products

Christiane Lorenz · Harald Hagendorfer · Natalie von Goetz · Ralf Kaegi · Robert Gehrig · Andrea Ulrich · Martin Scheringer · Konrad Hungerbühler

Received: 21 May 2010 / Accepted: 25 January 2011 / Published online: 12 February 2011

Abstract Consumer spray products are already on the market in the cosmetics and household sector, which suggest by their label that they contain engineered nanoparticles (ENP). Sprays are considered critical for human health, because the lungs represent a major route for the uptake of ENP into the human body. To contribute to the exposure assessment of ENP in consumer spray products, we analyzed ENP in four commercially available sprays: one antiperspirant, two shoe impregnation sprays, and one plant-strengthening agent. The spray dispersions were analyzed by inductively coupled plasma mass spectrometry (ICPMS) and (scanning-) transmission electron microscopy ((S)TEM). Aerosols were generated by using the original vessels, and analyzed by scanning mobility particle sizer (SMPS) and (S)TEM. On the basis of SMPS results, the nanosized aerosol depositing in the respiratory tract was modeled for female and male consumers. The derived exposure levels reflect a single spray application. We identified ENP in the dispersions of two products (shoe impregnation and plant spray). Nanosized aerosols were observed in three products that contained propellant gas. The aerosol number concentration increased linearly with the sprayed amount, with the highest concentration resulting from the antiperspirant. Modeled aerosol exposure levels were in the range of 10^{10} nanosized aerosol components per person and application event for the antiperspirant and the impregnation sprays, with the largest fraction of nanosized aerosol depositing in the alveolar region. Negligible exposure from the application of the plant spray (pump spray) was observed.

Keywords Consumer exposure · Spray products · Zinc oxide · Silver · Nanoparticles · Aerosol analysis · Health effects · EHS

Abbreviations

ENP	Engineered nanoparticles with diameter less than 100 nm
Spray dispersion	Low volatile substances of the spray products, left-over after evaporation of solvents due to

Electronic supplementary material The online version of this article (doi:10.1007/s11051-011-0256-8) contains supplementary material, which is available to authorized users.

C. Lorenz · N. von Goetz (✉) · M. Scheringer · K. Hungerbühler
Institute for Chemical and Bioengineering, ETH Zurich, Wolfgang-Pauli-Str. 10, 8093 Zurich, Switzerland
e-mail: Natalie.von.goetz@chem.ethz.ch

H. Hagendorfer · R. Gehrig · A. Ulrich
EMPA, Swiss Federal Laboratories for Materials Testing and Research, Ueberlandstrasse 129, 8600 Duebendorf, Switzerland

R. Kaegi
EAWAG, Swiss Federal Institute of Aquatic Science and Technology, Ueberlandstrasse 133, 8600 Duebendorf, Switzerland

	opening the original spray containers
Nanosized aerosol	Aerosol consisting of particles and droplets with diameter range of 10–100 nm

Introduction

Several hundreds of consumer products containing engineered nanoparticles (ENP) are on the market today, and their number is expected to increase rapidly in the near future. Silver, carbon, zinc oxide, titanium dioxide, and silica are the most regularly used materials, being incorporated in nanoparticular form into consumer products such as textiles, cosmetics, sports equipment, medical devices, food storage containers, and household chemicals (Nanotechproject 2008; Nanoforum 2006; Nielsen 2008). Among these products are ENP-containing and "nano"-labeled sprays in pump or propellant gas vessels. These sprays are expected to cause inhalation exposure resulting from the nanosized aerosol that is formed during product application.

Inhalation is considered as a critical uptake route for ENP (Kreyling et al. 2006; Maynard 2006; Oberdörster et al. 2005, 2007), because ENP can enter and be deposited in all parts of the respiratory tract. They diffuse through the thin alveolar membrane, reach the blood circulation system, and subsequently are transferred into various organs, as demonstrated recently for gold and titanium dioxide ENP (De Jong et al. 2008; Semmler-Behnke et al. 2008; Shin et al. 2010; Wu et al. 2009). Toxicological effects possibly include inflammatory response at the primary exposure sites in the alveoli (Lanone et al. 2009; Müller et al. 2010), as well as effects at secondary exposure sites such as internal organs (Wu et al. 2009). In the case of consumer sprays, ENP may reach the respiratory tract either as primary particles or as agglomerates/aggregates inside droplets of the inhaled aerosol.

Sprays usually release aerosols that can at least partly be inhaled by humans. Aerosols produced from consumer sprays have been analyzed in the micrometer range by Rogers et al. (2005) and Vernez et al. (2006). For waterproofing sprays, Yamashita and coworkers reported that in the micrometer range the particle diameter is related to the toxicity of the spray products (Yamashita et al. 1997). Other studies focused on household insecticides and exposure to biocide ingredients sprayed for disinfection of aeroplanes returning from tropical countries (Berger-Preiss et al. 2004, 2005, 2006).

Information about the nanosized aerosol fraction released from consumer sprays is however rare, and no studies about ENP-containing sprays on organic solvent-base, or sprays of complex composition have been published so far. In a recent study, we set up the experimental basis for the analysis of nanoparticles in water-based sprays and their aerosols (Hagendorfer et al. 2010). In this article, we present the extension of our method to organic solvent-based sprays and compare the aerosol generated by four commercially available sprays.

The aim of this study was therefore (i) to characterize the nanosized aerosol produced by commercial sprays, (ii) to compare the characteristics of the nanosized aerosol to the nanosized components found in the dispersions before spraying, and (iii) to model consumer exposure to nanosized aerosols released from the investigated sprays.

To address these aims, we analyzed the ENP content of the spray dispersions as well as particle and droplet size distributions between 10 and 500 nm in the aerosols of the spray products. The setup for the spray experiments was designed to represent the near-field breathing zone of a consumer. Based on the aerosol size distributions, a model of the exposure to nanosized aerosol was established, which uses specific parameters for the behavior of female and male consumers. Since the small ENP do not contribute to particle mass and at the same time toxic effects of ENP today are assumed to be correlated to measures other than mass (Wittmaack 2007; Dhawan et al. 2009), the exposure model is based on the number concentration and size of aerosol components instead of total particle mass. Furthermore, size-dependent deposition rates of ENP in the most relevant parts of the respiratory tract (alveolar, tracheobronchial, and nasal region) were included in the model (ICRP Publication 1994). This allowed us to model the number of nanosized aerosol components that deposit in the respiratory tract during one spraying event.

Experimental section and methods

Selection of spray products

Four commercially available products were included in this study: one antiperspirant spray (product I), two shoe impregnation sprays (products II and III), and one plant-strengthening agent (product IV); for an overview, see Table 1. Since specific information on ENP in the product description and ingredient declaration is rare, the criterion for product selection was that the packaging label contained either the term "nano", or a description implying that ENP could be present in the spray dispersion. Furthermore, only products were chosen that are freely available for the general population and that are proposed for consumer use, implying direct, near-field aerosol exposure during product application. According to the label and ingredients list, product I (antiperspirant) contained "antibacterial silver molecules" (label) and silver citrate (ingredients list). The "silver molecules" were described to have an antibacterial effect, and the product itself should provide a 24-h antitranspirant protection. The spray was marketed in a 150-mL spray vessel containing the propellant gases butane, isobutane, and propane. Products II and III (shoe impregnation sprays) were from the same brand and stated "nano" in the product name. The products were sold in propellant gas containers of 125 and 250 mL, respectively. No information about the propellant gases was given on the product packages of the two impregnation sprays. Product II was described to contain a UV-filtering component, and that "nano-particles" were forming an effective protective layer on the textile or leather, preventing dust adhesion. Product III was labeled as having a self-cleansing effect through nanotechnology, and, like product II, claimed that "nano-particles" would form a protective layer on the surface of the textile or leather. Product IV (plant spray) was labeled to contain "nano silver" in aqueous solution. The product was sold in a 500-mL pump spray vessel without propellant gas. The packaging information stated that regular usage of the spray prevented plants from being affected by bacteria, viruses, mold, fungus, or algae.

Analysis of dispersions

The propellant gas cans (products I-III) were cooled with liquid nitrogen for 5 min to ensure a secure opening of the pressurized containers. After opening the vessels, they were left over night at room temperature to guarantee complete evaporation of volatile substances. The remaining dispersions including non-volatile dispersant were collected without further dissolution and stored in the dark at 5°C. The dispersion of product IV, which was sold without propellant gas, could be collected without prior processing.

The spray dispersions were analyzed by inductively coupled plasma mass spectrometry (Agilent Technologies, Waldbronn, Germany, ICPMS 7500ce) for total concentrations of elements. Before analysis, the dispersions were dissolved by a microwave-assisted pressure digestion procedure (MLS, Leutkirch, Germany, 1200 MEGA microwave system, aqua regia or nitric acid, 40 min at 240°C, 250 mg sample weight).

In addition, dispersions were analyzed by (scanning) transmission electron microscopy ((S)TEM) in combination with an energy dispersive X-ray spectrometer (EDX) for determination of the morphology,

Table 1 Spray products analyzed in this study

No.	Product type	Product name	Manufacturer	Dispensing system	Information on package	Solvent
I	Antiperspirant	Nivea® Silver Protect	Beiersdorf	Propellant gas vessel	Silver molecules	Butane, isopropanol
II	Shoe impregnation spray	Nano Schmutz Blocker	Dosenbach, Ochsner AG	Propellant gas vessel	Nano	Organic
III	Shoe impregnation spray	Nano Wet Bloc	Dosenbach, Ochsner AG	Propellant gas vessel	Nano	Organic
IV	Plant strengthening agent	Nano-Argentum 10	NanoSys GmbH	Pump vessel	Nano-silver	Water

size distribution, and chemical composition of ENP. Samples were pipetted on TEM grids (copper 200 mesh with carbon film), soaked through with a lint-free tissue and left to dry at room temperature. (S)TEM investigations were performed on a Tecnai F30 microscope (FEI, Eindhoven, Netherlands, field emission cathode electron source, operated at 300 kV, point resolution ~2 Å). The (S)TEM images were recorded with a high-angle annular dark field (HAADF) detector using incoherently scattered electrons for image formation (Z contrast conditions). An EDX detector (AMETEK, Paoli, PA, United States) attached to the microscope allowed the analysis of the elemental composition of the samples. The electron micrographs were analyzed with the open source software ImageJ (NIOSH, United States). For analyzing the size distribution of particles in each sample, the size of at least 130 particles was measured from at least three different images. The ENP identified in the dispersions were of similar shape. Therefore, the mean and median size of ENP with relating standard deviation was determined.

Analysis of nanosized aerosols

The samples were dispensed with their original spray vessels in a glovebox equipped with a high-efficiency particulate air (HEPA) filter and a ventilation unit (Mecaplex, Grenchen, Switzerland, dimensions 94 × 55 × 67 cm (b, l, h), volume of 300 L). The setup ensured a low particle background by active filtering between sampling and a standardized environment for reliable simulation experiments. For a schematic illustration of the measurement setup, see Fig. 1.

The goal was to simulate an untreated aerosol as inhaled by consumers with the glovebox dimensions reflecting the near-field breathing zone of a consumer. Hence, the aerosols were generated with the original spray containers at room temperature. The size distribution and the particle number concentration of the nanosized aerosols were monitored with a scanning mobility particle sizer (TSI GmbH, Aachen, Germany, SMPS 3034) and an electrostatic sampler for (S)TEM analysis (design described in Fierz et al. 2007). The transfer lines connecting the glovebox with the measuring devices consisted of Tygon® with an inner diameter of 0.5 cm and a length of 50 cm. Transfer diffusion losses were calculated according to Willeke and Baron (1993) and were 6 and 0.3% for particle diameter of 10 and 100 nm, respectively. A more detailed description of the method development, reproducibility, and accuracy of the set-up is given in Hagendorfer et al. 2010.

As soon as the background in the glovebox was stable (measured with SMPS), the ventilation was turned off. Hence, no air-flow could influence the distribution of the aerosol in the glovebox, except for the draw of the SMPS and electrostatic sampler (1.5 L/min). The sprays were manually dispersed into the glovebox at the start of an SMPS run (sampling scan starts with the smallest SMPS size fraction). Then, two consecutive SMPS scans were recorded. For the list of size fractions sampled by SMPS within 100 s, see Table S1 in supplementary information. The spray vessels were weighed before and after spraying on a precision weighing module (Mettler, Greifensee, Switzerland, PM 6100) to determine the weight loss of the spray can, i.e., the amount of the dispersion that was dispersed. Per product, we sprayed for 1–5 s, which represented sprayed masses between 0.2 and 3.5 g. The aerosol background number concentration was subtracted before the

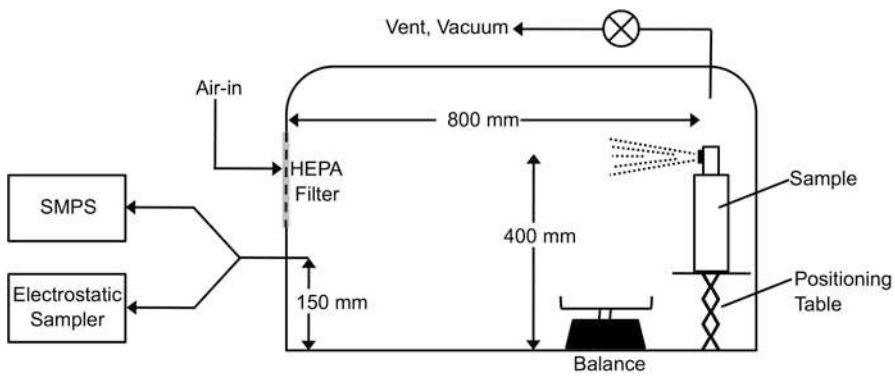

Fig. 1 Schematic representation of the sampling setup

analysis of results. The sampling with the electrostatic sampler continued for 60 min, with seven spraying events each lasting 1 s, in regular time intervals. The images were analyzed with the open software ImageJ. Per spray product, sample at least 50 particles were measured from at least three different images. In contrast to the particles identified in the dispersions before spraying, the particles identified in the aerosols were of different shapes and broader size range. The mean value is therefore dominated by the large particles. Thus, the size range and median diameter are given instead.

Modeling exposure to nanosized aerosols

The exposure levels modeled in this study reflect the nanosized aerosol that deposits in either the alveolar, tracheobronchial, and nasal region in the respiratory tract after a single application of the respective spray. As an exposure model, we used an adaptation of the model proposed by the European Chemicals Agency (ECHA) for assessing inhalation exposure under REACH (ECHA 2008, Chapter R.15: Consumer exposure estimation; Equation 15-2). As, for nanoparticles, the mass is not a suitable measure, the model is based on particle number instead of mass.

First, the aerosol number concentrations measured in our glovebox experiment (Fig. 1) were extrapolated to match sprayed amounts that are applied by consumers during a single spray event (for values see Table 2 input parameter "*spray amount*"). The amounts, a_{spray}, represent worst case amounts as reported for antiperspirant in RIVM report (2006) and for shoe impregnation in Engelund and Sørensen (2005). The amount reported for the antiperspirant is gender independent, whereas the amount for shoe sprays differs for female and male consumers, since shoes of men are on average larger than shoes of women. For extrapolation, Eq. 1 was used along with the specific regression coefficients, m and n, that were derived from spray experiments with varying spray amounts (see Table S2 in supplemental information). The linear regressions are shown in Fig. 2. The transfer diffusion losses in the experimental setup were neglected in this model step, because they were <6% (see supplemental information SI).

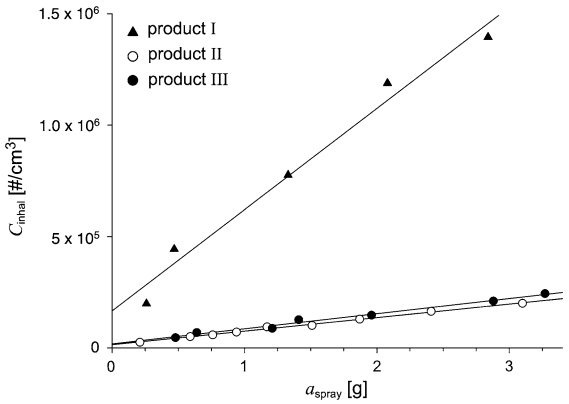

Fig. 2 Nanosized aerosol number concentrations of products *I–III* as measured by SMPS against the sprayed amount, a_{spray}. Product *IV* resulted in a nanosized aerosol number concentration not exceeding the background level, independent of the sprayed amount

$$C_{inhal}(a_{spray}) = m \cdot a_{spray} + n \quad (1)$$

where, C_{inhal} is the number concentration of nanosized aerosol during application of spray amount a_{spray}, a_{spray} is the spray amount reported in literature [g], and m, n are the regression coefficients [−].

In step two, the total aerosol concentrations obtained through step one, C_{inhal}, were divided into the 32 SMPS size fractions between 10 and 100 nm, j. Owing to the long measuring time of the SMPS (3 min from 10 to 500 nm), we concentrated the modeling on the fraction between 10 and 100 nm (collected in the first 100 s).

Table 2 Model input parameters used for modeling the exposure to nanosized aerosols

Input parameter	Product I	Product II	Product III
ENP conc., C_{inhal} [#/cm^3]	1.98 × 10^6	7.84 × 10^5 (f)/1.14 × 10^6 (m)	8.79 × 10^5 (f)/1.28 × 10^6 (m)
Spray amount, a_{spray} [g]	4	12.65 (f)/18.48 (m)	12.65 (f)/18.48 (m)
Respirable fraction, F_{resp} [−]	1	1	1
Inhalation rate, IH_{air} [cm^3/min]	8630 (f)/10650 (m)	8630 (f)/10650 (m)	8630 (f)/10650 (m)
Total exp. time, $t_{contact}$ [min]	5	8	8

References for the parameters see text

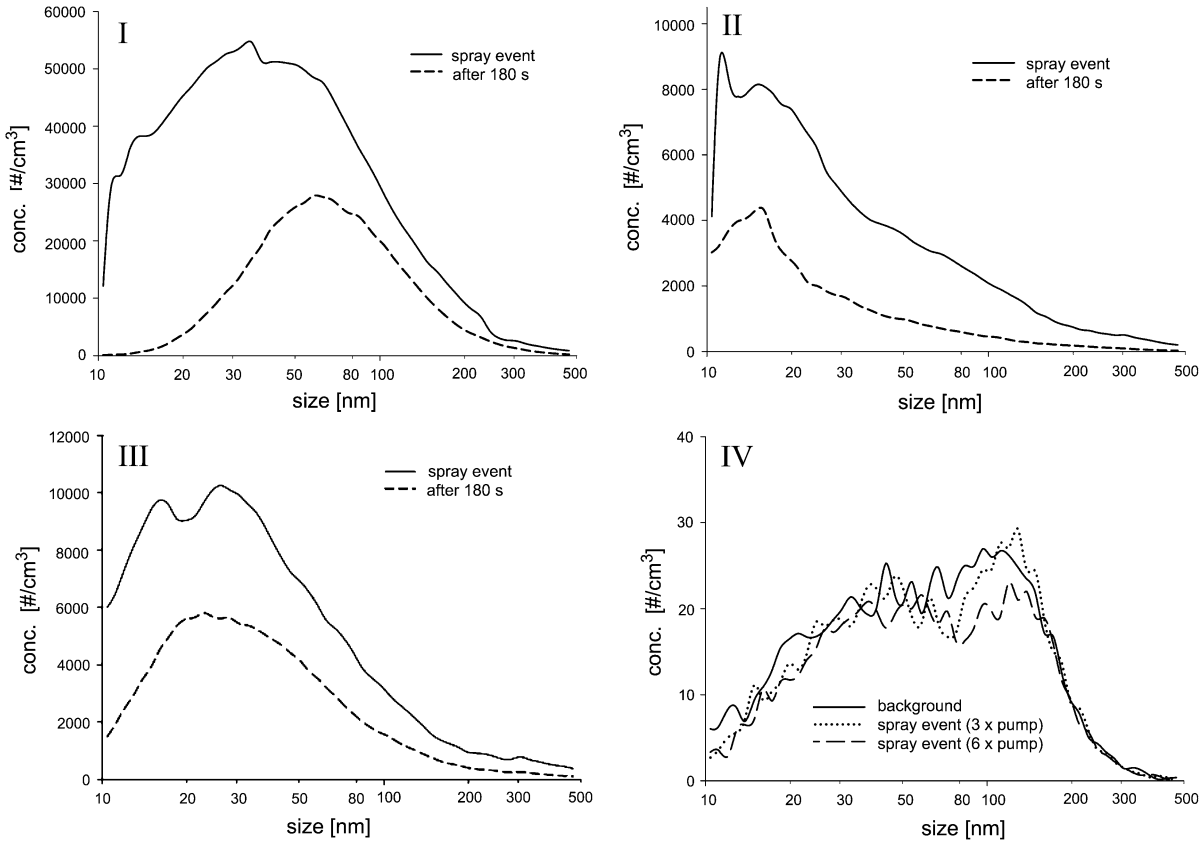

Fig. 3 Size distributions of the aerosol as determined in the spray experiments used for modeling exposure to products *I–III* (background-corrected) and consecutive scans. For product *IV* size distributions for different spray amounts (not background-corrected) and background are shown

Nevertheless, scans were always recorded up to 500 nm. It was assumed that the size distribution of total C_{inhal} is always the same as found for the highest spray amount analyzed during the spray experiments (see Fig. 3 for illustration of size distributions). Each SMPS size fraction, *j*, represents one of the size fractions separated by the used instrument. The differentiation of SMPS size fractions was necessary to be able to account for size-dependent deposition rates in the model. For the list of size fractions, see Table S1 in supplemental information.

Equation 2 was then used for each of the size fractions separately, to model the nanosized aerosol depositing in either the nasal, tracheobronchial or alveolar region, respectively. The input parameters used in Eq. 2 are shown in Fig. 4 (deposition rates according to ICRP Publication 1994) and Table 2 (other parameters). Further, it was distinguished between female and male consumers, because they show different body characteristics and application behavior. First, the inhalation rates are gender specific (females inhale on averages less air than males). Second, the foot size was assumed to be different, which has direct influence on how much impregnation spray is used to fully treat one pair of shoes.

$$E_{\text{j\_region}} = C_{\text{inhal}_{\text{j\_region}}} \cdot r_{\text{dep}_{\text{j\_region}}} \cdot F_{\text{resp}} \cdot IH_{\text{air}} \cdot t_{\text{contact}} \quad (2)$$

where $E_{\text{j\_region}}$ is the nanosized aerosol deposition of SMPS size fraction *j*, in either the alveolar, tracheobronchial, or nasal region [#], $C_{\text{inhal}_{\text{j\_region}}}$ the number concentration of ENP size fraction in aerosol, based on analysis by SMPS [#/cm^3], $r_{\text{dep}_{\text{j\_region}}}$ the deposition fraction of respective ENP size fraction according to ICRP model, not gender specific [−], F_{resp} the respirable fraction of nanosized aerosol [−], IH_{air} the inhalation rate of female or male consumer

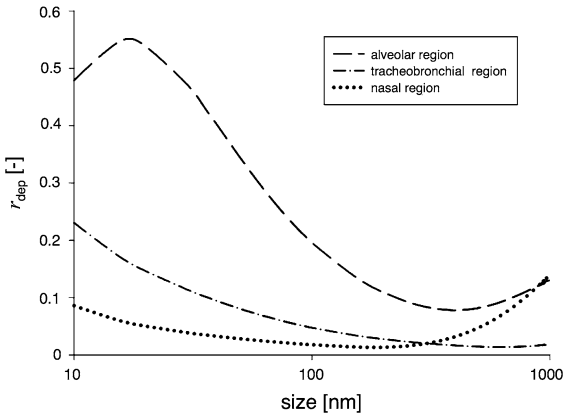

Fig. 4 ICRP deposition fraction (ICRP Publication 1994) used as r_{dep} in the model. For a better overview, deposition fractions for particles up to 1000 nm are shown

[cm^3/min], and $t_{contact}$ is the exposure time per application event [min].

The deposition rates, r_{dep}, were based on the ICRP model (ICRP Publication 1994) that gives size-specific deposition rates for three regions (alveolar, tracheobronchial, or nasal region) within the respiratory tract. The deposition rates were assumed to be the same for female and male consumers. The aerosol number concentrations, C_{inhal}, were the extrapolated experimental results obtained from aerosol analysis by SMPS and obtained in step one of the modeling procedure. The respirable fraction of nanosized aerosol, F_{resp}, was set to one in the model, because ENP smaller than 100 nm can potentially reach all parts of the respiratory tract. As inhalation rates, IH_{air}, typical values for minor physical work in standing position were used for female and male consumers, respectively (Trudel et al. 2008). The total exposure time, $t_{contact}$, denotes the time a consumer is in contact with the aerosol during and after the spray application. For the antiperspirant, a worst case value reported in RIVM report (2010) was used. For the application of shoe sprays, the mean value reported for the spraying time of the US citizens in USEPA (1997) was rounded up to 8 min. The aerosol concentration was assumed to be constant over the course of 8 min (continuous spraying).

As a third step, for each of the regions, the deposited particle numbers in all 32 SMPS size fractions were summed up according to Eq. 3 to obtain the total region-specific exposure level.

$$E_{dep\_region} = \sum_{j=1}^{32} E_{j\_region} \quad (3)$$

where E_{dep_region} is the nanosized aerosol deposition in the alveolar, tracheobronchial, or nasal region, respectively [#], and j SMPS size-fraction.

Modeling was carried out in three steps and based on Eq. 1–3. The model uses the maximum resolution of the experimental data: results from all SMPS size fractions were modeled separately, each with their respective aerosol number concentration and with size-related, region-specific deposition rates.

General assumptions of our exposure model were an evenly distributed aerosol concentration within the glovebox (i.e., no spatial gradient), because the aerosol was sampled at only one place, and that the inhalable aerosol concentration and consumer inhalation rates remained constant during the whole contact time.

Results

Analysis of spray products

An overview of results obtained from analyzing the spray dispersions and aerosols of products I–IV is provided in Table 3. The particle size distributions that were used for modeling are illustrated in Fig. 3. The plots include also the consecutive scan recorded after 180 s, demonstrating the aerosol evolution with time. Representative electron micrographs are illustrated in Fig. 5. A detailed description of the analytical results is provided in Table 3 for each product separately. EDX spectra of samples and SMPS size distributions of various spray amounts are provided in the SI.

Product I (antiperspirant)

In the dispersion, 6.8 ± 0.7 mg silver/kg was determined by ICPMS. On TEM micrographs (see Fig. 5Ia), structures in the micrometer-range are visible, but ENP with a diameter smaller than 100 nm could not be identified. In contrast to the ICPMS results, no silver was detected by EDX. The absence of silver may be due to the very low silver concentration (<10 mg/kg), or to

Table 3 Analytical results for spray dispersion and spray aerosol analysis, listed by product number

No.	Dispersion				Aerosol			
	TEM			ICPMS	TEM			SMPS
	Shape	Average size ± SD (median diameter)	Elements detected by EDX	mean ± SD	Shape	Size range (median size)	Elements detected by EDX	mode ± SD[c]
I	Various	Structures in μm range	Al, C[a], Cl, Mg, O, Si, Cu[a]	6.8 ± 0.7 mg/kg Ag	Round Longish	3–78 nm (18 nm) Length 55–154 nm (72 nm) Width 10–25 nm (17 nm)	Al, C[a], Ca, Cl, Mg, O, Si, Cu[a]	Broad size distribution without clear maximum 35.2 ± 2.2 nm
II	Roundish	23 ± 8 nm (22 nm)	C[a], Cl, F, O, Zn, Cu[a]	470 ± 10 mg/kg Zn	Roundish	4–4300 nm (43 nm)	C[a], Cl, F, O, Zn, Cu[a]	Maximum at size <15 nm 11.1 ± 2.3 nm
III	None	No particles visible	C[a], Cl, F, O, Cu[a]	No significant amount of metal(–oxides) detected	Roundish	32–3230 nm (305 nm)	C[a], Cl, F, O, Cu[a]	Broad size distribution without clear maximum 26.4±2.2 nm
IV	Roundish	8 ± 6 nm (8 nm)	Ag, C[a], O, Si, Cu[a]	9.1 ± 0.1 mg/kg Ag	Not collected[b]			Signal similar to background level

[a] Signal due to TEM grid

[b] Results from SMPS aerosol analysis showed the absence of particles/droplets in the nanometer range

[c] Values are given for the size distributions used for modeling

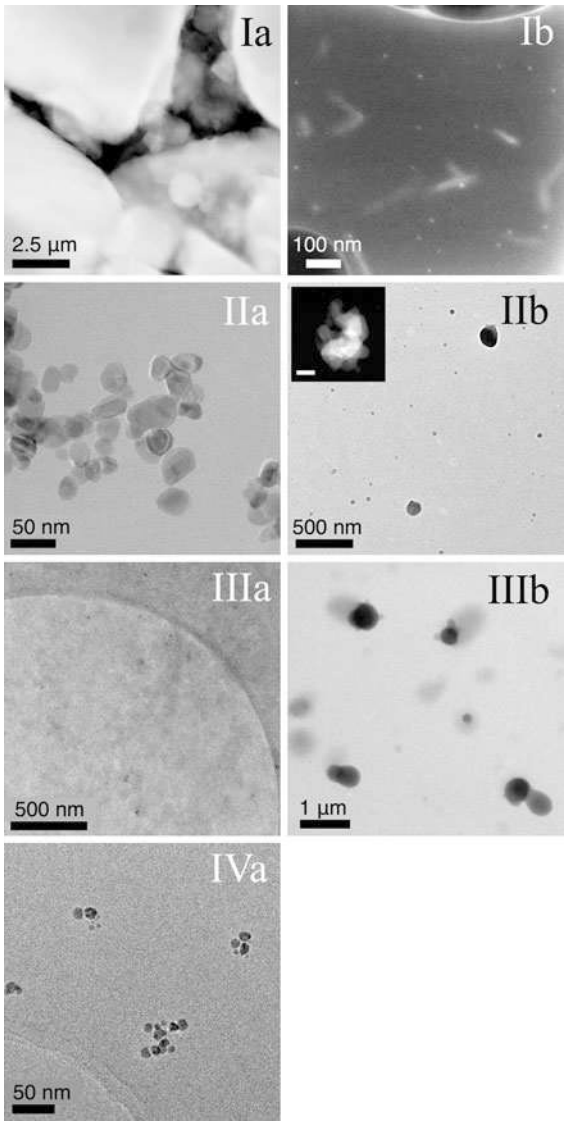

Fig. 5 Transmission electron micrographs of products *I–IV*. Per product, images are arranged horizontally, with the image of the dispersion on the left (**a**) and the image of the aerosol on the right (**b**). Images of one product can therefore be compared horizontally; images of the dispersion and aerosol of different products can be compared vertically. No TEM image of the aerosol of product IV is shown, as SMPS results attested the absence of a nanosized aerosol. *Scale bar* in the inset of image *IIb* is 500 nm

silver being present in the ionic form, rather than as particles consisting of elemental silver.

Spraying of product I resulted in a nanosized aerosol with mode at 35.2 ± 2.2 nm (mode ± SD) (see Fig. 3I). The consecutive scan shows that the maximum of the curve is shifted to larger size fractions with mode at 54.2 ± 1.9 nm. The aerosol number concentration was found to depend linearly on the amount sprayed (see Fig. 2). According to the regression in Fig. 2, spraying 1 g of the dispersion resulted in an aerosol number concentration of 6.2×10^5 per cm^3. For the size distributions of all spray amounts, see Fig. S11 in supplemental information. For all spray amounts, it was found that within the analyzed particle size range of 10–500 nm, 86–91% of the particles were smaller than 100 nm.

Owing to overload of the sampling device for product I we could not use the electrostatic sampler. Thus, the aerosol of product I was collected by placing a TEM grid at 20 cm distance from the spray nozzle for one second during spraying. On TEM images (see Fig. 5Ib, aerosol) two types of particles in the nanometer range could be identified: round particles with diameters between 3 and 78 nm (median diameter 18 nm), and longish particles with median dimensions of 17 × 72 nm. By elemental analysis, again no silver was detected, presumably for the same reasons as for the dispersion. Instead, aluminum, calcium, chlorine, magnesium, oxygen and silicon were detected, implying that the particles visible on the images consist of spray ingredients listed on the package such as cyclomethicone (silicon, oxygen), aluminum chlorohydrate (aluminum, chlorine, oxygen) or disteardimonium hectorite (magnesium, silicon, oxygen, etc.).

Product II (shoe impregnation)

By ICPMS, the total concentration of zinc was determined as 470 ± 10 mg zinc/kg, corresponding to 584 ± 12 mg zinc oxide/kg. On the TEM images (see Fig. 5IIa), primary particles of 23 ± 8 nm (mean ± SD) were observed. In accordance with the ICPMS results, elemental EDX analysis confirmed zinc and oxygen as the main elements, suggesting that the ENP visible in the electron micrographs consisted of zinc oxide (ZnO). The primary particles can be clearly recognized as separate, non-agglomerated entities. However, the particles seem to be loosely grouped, which could be an effect of sample preparation (vessel cooling, opening, and drying of dispersion on TEM grid). Large particle aggregates were not visible. By EDX chlorine and fluorine were detected, suggesting that

acrylate polymers with chlorine and fluorine are present in product II, which are used in impregnation sprays because of their water-repellent properties.

Spraying of product II produced a nanosized aerosol with the maximum at small size fractions <15 nm. The size distribution taken for modeling had its mode at 11.1 ± 2.3 nm (see Fig. 3II, aerosol). After 180 s, the consecutive scan shows a mode at a higher size fraction (16 ± 1.7 nm).

The aerosol number concentration for 1 g of the sprayed dispersion was 7.6×10^4 per cm^3. For the different spray amounts, the aerosol number concentration was found to increase linearly with amount dispensed (see Fig. 2). For the size distributions of different spray amounts, see Figure S12 in supplemental information. Similar to product I, the majority of aerosol components (90–93%) that were detected by SMPS were smaller than 100 nm.

TEM images of product II (see Fig. 5IIb) show mostly roundish particles, but also particles of various other shapes with a broad size distribution between 4 and 4300 nm, whereas the majority of particles was observed in the lower nanometer range <100 nm (median diameter 43 nm). Zinc and oxygen were detected by EDX, as well as chlorine and fluorine. The zinc signal was however only observed for particles in the micrometer range, suggesting that the ZnO ENP were present solely in large particles. The particles <100 nm are therefore likely to consist of acrylate polymers. It could not be verified in which form the ZnO was present within the large particles.

Product III (shoe impregnation)

No metals and elements commonly used as nanoparticles were detected by ICPMS. By TEM analysis, no particles in the nano- or micrometer range were found in the electron micrographs (see Fig. 5IIIa). Elemental EDX analysis showed chlorine and fluorine. The results of ICPMS and EDX lead to the assumption that no metal or metal oxide ENP were present in the dispersion of product III.

Spraying of product III resulted in a broad size distribution smaller than 100 nm. The size distribution included in the modeling had its mode at 26.4 ± 2.2 nm (see Fig. 3III). In the consecutive scan that describes the aerosol concentration with a time shift of 3 min, the mode is slightly shifted toward a smaller size fraction of 22.9 ± 2.0 nm. This is within the measurement error, but might indicate that particles <10 nm (that are not assessed with our measurement device) agglomerate to particles >10 nm and thus contribute to the fraction of very small particles. Spraying 1 g of the dispersion resulted in a nanosized aerosol number concentration of 8.6×10^4 per cm^3. It has to be highlighted that product II, which contains ENP in the spray dispersion, results in a slightly lower aerosol number concentration than product III that can be assumed to contain no metal (-oxide) ENP in the dispersion. Like for products I and II, the aerosol number concentration of product III was found to increase linearly with spray amount (see Fig. 2). Considering the measurement error of the SMPS the size distributions can be regarded as being similar irrespective of the spray amount (for SMPS electropherograms see Figure S13 in supplemental information). The majority of aerosol components detected by SMPS were, like for the other products, smaller than 100 nm (90–93%). TEM images of product III (see Fig. 5IIIb, aerosol) show, similar to product II, mostly roundish particles with a broad size distribution between 32 and 3230 nm. Chlorine and fluorine were detected by EDX, which suggests that the aerosol particles consist of acrylate polymers.

Product IV (plant treatment)

A concentration of 9.1 ± 0.1 mg silver/kg was determined by ICPMS. The TEM images showed round particles of 8 ± 6 nm (see Fig. 5IVa). Elemental EDX analysis confirmed the presence of silver as the main component of the particles.

Spraying of product IV resulted in SMPS signals similar to the background signal irrespective of the dispensed spray amount (see Fig. 3IV). The two scans that illustrate the spray events have modes at 129 ± 2.2 nm and 120 ± 2.2 nm, respectively. Comparison between the number of aerosol components smaller than 100 and 500 nm showed that 68–70% were smaller than 100 nm. This ratio is similar to the one of the background aerosol, where 71% of the aerosol components were smaller than 100 nm.

Because the aerosol concentration was found to be similar to the background level, no samples were collected with the electronic particle sampling technique.

The fact that the measured aerosol number concentration up to 500 nm did not exceed the background concentration does not mean that during a spray event of product IV no aerosol is released at all. Rather, it is likely that the aerosol droplets generated with the pump spray vessel were so large that they were deposited either on the floor by gravity or on the walls of the glovebox. It was clearly visible that the aerosol wetted the glovebox and the beginning of the tubing.

Aerosol exposure levels

Figure 6 illustrates the exposure levels resulting from a single application of products I–IV, i.e., the nanosized aerosol that deposits in three regions of the respiratory tract (exposure levels listed in Table 4). Products I–III result in exposure levels in the order of 10^{10} aerosol components in the whole respiratory tract, whereas the application of product IV results in exposure similar to background level. For products I–III, male consumers (m) experience higher exposure than females (f). The gender difference was more pronounced for the impregnation sprays (products II and III). The difference originates from the fact that male consumers on average use more impregnation spray per pair of shoes than female consumers because their shoes are larger. Moreover, male consumers have usually a higher inhalation rate than female consumers. In all the cases, the majority of the nanosized aerosol deposits in the alveolar region (highlighted in black), whereas the least deposit in the nasal region.

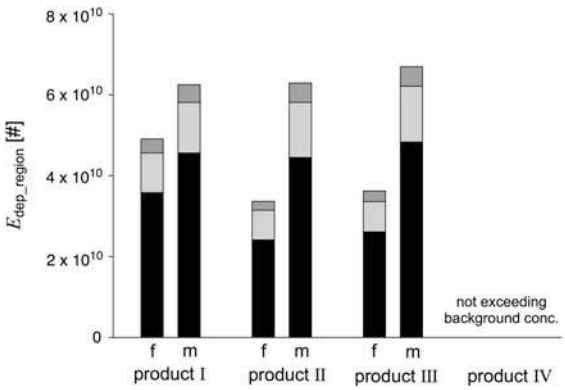

Fig. 6 Exposure levels, E_{dep}, resulting from the application of products *I–IV*, based on aerosol concentrations analyzed by SMPS. Results are illustrated for female (*f*) and male (*m*) consumers, for the alveolar (*black*), tracheobronchial (*light gray*), and nasal (*dark gray*) region

Discussion

The ENP could clearly be identified in the dispersions of products II and IV, but not in the dispersions of products I and III. Nanosized aerosol number concentrations that were significantly higher than the background concentrations were identified for products I–III. The nanosized aerosols consisted of a mixture of the respective spray ingredients. The ENP identified in the dispersion of product II, however, were not homogenously distributed within the droplets and particles of the aerosol. By EDX, zinc signals were obtained solely in particles greater than 100 nm. Further, the zinc signal was found always in combination with fluorine and chlorine signals. We therefore assume that the ZnO-ENP mostly agglomerate in the aerosol and are surrounded by an acrylate polymer matrix. Thus, ENP can enter the respiratory tract of consumers as parts of aerosol components in the micrometer range. These aerosol components may (a) consist of a hardened polymer containing ZnO-ENP or (b) droplets that contain both free ZnO-ENP and polymer particles with or without ZnO-ENP. For the first case, ZnO-ENP will only get in contact to lung cells if the polymer matrix is

Table 4 Modeled exposure levels as illustrated in Fig. 6

No.	$E_{dep\_alveolar}$ [#]		$E_{dep\_tracheobronchial}$ [#]		E_{dep_nasal} [#]	
	Female	Male	Female	Male	Female	Male
I	3.6×10^{10}	4.6×10^{10}	9.8×10^{9}	1.3×10^{10}	3.5×10^{9}	4.4×10^{9}
II	2.4×10^{10}	4.5×10^{10}	7.4×10^{9}	1.4×10^{10}	2.6×10^{9}	4.8×10^{9}
III	2.6×10^{10}	4.8×10^{10}	7.5×10^{9}	1.4×10^{10}	2.6×10^{9}	4.9×10^{9}
IV	Similar to background exposure					

dissolved. For the latter case, the ZnO-ENP will reach the lung cells transported by the microsized droplets and can directly act on the cells.

Product I and III both produced nanosized aerosols after spraying, even though we did not detect any ENP in the dispersions of these products. Consumers applying these products are therefore expected not to get in contact with any ENP, but with nanosized aerosol components that are generated during the spraying process. As identified by EDX, these nanosized components consist of a mixture of spray ingredients present in the dispersion, e.g., of hardened polymer for product III.

Because both, ENP-containing product II as well as ENP-free products I and III, generated nanosized aerosols, we conclude that the ENP contained in the dispersion of product II have no significant influence on the generated aerosol number concentration. However, further experiments with ENP-containing sprays in comparison to ENP-free sprays of the same composition are needed to prove this hypothesis.

In the case of product IV, the nanosized aerosol concentration after spray events was similar to the background concentration. We therefore conclude that the spraying of product IV does not generate a measurable fraction of nanosized droplets, even though the spray dispersion contains ENP. The ENP are expected to be part of aqueous droplets with such a large diameter and high mass that they settle down in the analytical setup, before they can reach the sampling equipment.

The main differences between products I–III (producing nanosized aerosol) and product IV (with no measurable concentration of nanosized aerosol) were the design of the spray containers and the composition of the dispersions. Products I–III were sold in pressurized containers and contained propellant gas and solvent, whereas product IV was on aqueous basis and sold in a pump vessel without propellant gas. It was demonstrated in a previous study that the number concentration and aerosol size distribution is influenced by the design of the dispensing system (Hagendorfer et al. 2010).

It is therefore expected that also for products I–IV the aerosol properties depend both on the design of the spray can and the composition of the dispersion. With our experiments their influence cannot be separated. Spray dispersions and spraying devices, however, mutually depend on each other and are designed to meet the purpose of the respective product. From the multitude of possible combinations only those that are actually used in the market are relevant for the consumers. Therefore, by focusing on commercially available products in original containers, we were able to derive realistic exposures for consumers.

The method that was used for both assessing the size distribution of ENP in the aerosol and in the dispersion was that of (S)TEM. An important disadvantage of this method is that ENP can only be analyzed in the dry state, i.e., it is not possible to analyze the dispersions as they are present in the vessels. The processing of the dispersions can induce artifacts such as aggregation or agglomeration of the primary particles. Therefore, samples were not diluted or sonicated before analysis by (S)TEM.

Other potentially suitable techniques such as dynamic light scattering (DLS), multi-angle light scattering (MALS), or X-ray diffraction (XRD), work only for particles with similar shape and narrow size distribution. Because the properties of particles in this study were not known beforehand, and because some samples proved to contain particles of a large size distribution, electron microscopy was considered to be a suitable method.

The spray experiments were carried out in a glovebox with a volume of 300 L in total, which was connected to an SMPS device. Because the aerosol passed a tubing of 50 cm from the glovebox to the SMPS, a fraction of the nanosized aerosol deposits or adsorbs within the tubing. This leads to a small underestimation of the measured number concentrations. On the basis of device dimensions, we estimated that the particle loss is 0.3–6% for particles with diameter between 10 and 100 nm, respectively. For detailed calculations on particle loss, see SI.

During the spray experiments, no ventilation was used. This does not represent the typical real-life surroundings of consumers when using sprays, especially not for shoe sprays that should be used outdoors. The volume in which the aerosol is dispensed is normally several cubic meters, with air exchange due to room ventilations (e.g., in bathrooms), open windows or doors, or wind. In the relatively small volume of the used glovebox, the wall deposition rate might be enhanced as compared to a normal room.

Environmental factors such as temperature and humidity may additionally have an influence on the

aerosol in terms of time needed for solvent evaporation, agglomeration processes, and settling of particles.

The SMPS used in the spray experiments needs more than one minute to scan from 10 to 100 nm. The properties of the aerosol, however, change with time. Droplets may evaporate and become smaller with time. Within the same time span, droplets may agglomerate and form droplets with increased size. We have demonstrated that, after 180 s, the aerosol number concentration for products I–III decreases significantly. We assume therefore that the measurable aerosol number concentration decreases with time, hence that the number concentration of the large size fractions in the SMPS diagrams are underestimated. However, because all products were analyzed by exactly the same setup, every SMPS scan includes the same time factor. It can therefore be concluded that the results are intercomparable in this respect.

Within the glovebox, the sprays were dispensed in the direction of the sampling site. In everyday life, however, products II–IV are usually not sprayed directly into the face. Only product I (antiperspirant) is directed toward the body during a usual spraying event. The aerosol number concentrations measured within the glovebox should therefore be regarded as relatively high concentrations. Other model input parameters concerning consumer behavior and body characteristics reflect realistic worst-case assumptions.

The reported exposure levels have to be seen in the context of general particle exposure. Consumers are exposed to manifold particle types from different sources during everyday life such as vehicle exhaust, house dust, or cigarette smoke. These particles differ in composition, size, shape, and other properties. Ambient aerosols hence contain nanosized as well as micrometer-sized components, with inhalation exposure being an everyday phenomenon. For example, air can contain 10^3–10^5 particles per cm^3 (Aalto et al. 2005; Matson 2005; Zhu et al. 2009), and activities such as candle burning or cooking may even induce concentrations of up to 10^4 and 10^{12} particles per cm^3 air, respectively (Wallace et al. 2004; Matson 2005; Buonanno et al. 2009). The aerosol concentrations from propellant gas cans that were analyzed within this study contained 10^4–10^6 particles per cm^3 air and are therefore in a similar range as the other particle sources described above. However, the properties and the chemical identity of the particles are different in these sources, and it remains to be investigated whether the ENP from sprays induce the same effects as other ambient particles.

Conclusion

The analysis of commercially available spray products showed that products labeled to contain "nano-particles" or "molecules" do not necessarily contain ENP in the spray dispersion. We identified two spray products containing ENP in the dispersions, which are commercially available to the general population in Switzerland and Germany. However, during any spraying event, nanoparticles can be generated irrespective of ENP contained in the original dispersion. These consist, e.g., of fluorocarbons that may have comparable toxicological effects as suspected for ENP.

In future studies, focus should be laid upon the investigation of aerosol concentrations in real-life environments. Important factors in this respect are humidity, co-use of different products (mixing of different aerosols), and behavior of aerosols in larger volumes. In addition, toxicological studies are of importance, investigating the interaction between ENP and lung cells, ENP uptake rates into the human body, and the ENP distribution within the organism. Such data will allow for more detailed modeling of aerosol exposure, including uptake into and impact of nanosized aerosols on the human body.

Acknowledgments Funding by the Swiss Federal Institute of Public Health is gratefully acknowledged (Grant No. 06.001691). The authors would like to thank F. Krumeich for TEM and EDX analysis performed at the EMEZ (Electron Microscopy Center of the ETH Zürich), and C. Nickel from the Institute of Energy and Environmental Technology e.V., Germany, for providing data on particle deposition rates.

References

Aalto P, Hämeri K, Paatero P, Kulmala M, Bellander T, Berglind N, Bouso L, Castano-Vinyals, Sunyer J, Cattani G et al (2005) Aerosol number concentration measurements in five European cities using TSI-3022 condensation particle counter over a three-year period during health effects of air pollution on susceptible subpopulation. J Air Waste Manage Assoc 55(8):1064–1076

Berger-Preiss E, Koch W, Behnke W, Gerling S, Kock H, Elflein L, Appel KE (2004) In-flight spraying in aircrafts:

determination of the exposure scenario. Int J Hyg Environ Health 207(5):419–430
Berger-Preiss E, Boehncke A, Koennecker G, Mangelsdorf I, Holthenrich D, Koch W (2005) Inhalational and dermal exposures during spray application of biocides. Int J Hyg Environ Health 208(5):357–372
Berger-Preiss E, Koch W, Gerling S, Kock H, Klasen J, Hoffmann G, Appel KE (2006) Aircraft disinsection: exposure assessment and evaluation of a new pre- embarkation method. Int J Hyg Environ Health 209(1):41–56
Buonanno G, Morawska L, Stabile L (2009) Particle emission factors during cooking activities. Atmos Environ 43(20): 3235–3242
De Jong WH, Hagens WI, Krystek P, Burger MC, Sips AJAM, Geertsma RE (2008) Particle size-dependent organ distribution of gold nanoparticles after intravenous administration. Biomaterials 29(12):1912–1919
Dhawan A, Sharma V, Parmar D (2009) Nanomaterials: a challenge for toxicologists. Nanotoxicology 3(1):1–9
ECHA (2008) Guidance on information requirements and chemical safety assessment. Chapter R.15. In: Consumer exposure estimation. Version 1.1 Available from the website http://guidance.echa.europa.eu/docs/guidance_document/information_requirements_en.htm. Accessed May 2010
Engelund B, Sørensen H (2005) Mapping and health assessment of chemical substances in shoe care products. Danish Ministry of the Environment. Environmental Protection Agency. Survey of Chemical Substances in Consumer Products. No. 52 2005
Fierz M, Kaegi R, Burtscher H (2007) Theoretical and experimental evaluation of a portable electrostatic TEM sampler. Aerosol Sci Technol 41(5):520–528
Hagendorfer H, Lorenz C, Kaegi R, Sinnet B, Gehrig R, Goetz Nv, Scheringer M, Ludwig C, Ulrich A (2010) Size-fractionated characterization and quantification of nanoparticle release rates from a consumer spray product containing engineered nanoparticles. J Nanopart Res 12(7): 2481–2494
ICRP Publication 66 (1994) Human respiratory tract model for radiological protection. A report of a Task Group of the International Commission on Radiological Protection. Ann ICRP 24(1–3):1–482
Kreyling WG, Semmler-Behnke M, Möller W (2006) Health implications of nanoparticles. J Nanopart Res 8(5):543–562
Lanone S, Rogerieux F, Geys J, Dupont A, Maillot-Marechal E, Boczkowski J, Lacroix G, Hoet P (2009) Comparative toxicity of 24 manufactured nanoparticles in human alveolar epithelial and macrophage cell lines. Part Fibre Toxicol 6(14):1–12
Matson U (2005) Indoor and Outdoor concentration of ultrafine particles in some Scandinavian rural and urban areas. Sci Tot Environ 343(1–3):169–176
Maynard A (2006) Nanotechnology: assessing the risks. Nanotoday 1(2):22–33
Maynard A, Aitken RJ (2007) Assessing exposure to airborne nanomaterials: current abilities and future requirements. Nanotoxicology 1(1):26–41
Müller L, Riediker M, Wick P, Mohr M, Gehr P, Rothen-Rutishauser B (2010) Oxidative stress and inflammation response after nanoparticle exposure: differences between human lung cell monocultures and an advanced three-dimensional model of the human epithelial airways. J R Soc Interface 7(6):S27–S40
Nanoforum (2006) European Nanotechnology Gateway. Nanoforum Report: Nanotechnology in consumer products. 9th General Report. Available from the website: http://www.nanoforum.org. Accessed October 2006
Nanotechproject (2008) Woodrow Wilson International Centre for Scholars. Project on Emerging Nanotechnologies. Consumer products inventory of nanotechnology Products. Available from the website: http://www.nanotechproject.org/inventories/consumer/analysis_draft/. Accessed August 2009
Nielsen E (2008) Nanotechnology and its impact on Consumers. EBN Consulting. Report to the Consumer Council of Canada. Available from the website: http://www.consumercouncil.com/index.cfm?pid=20399. Accessed July 2009
Oberdörster G, Maynard A, Donaldson K, Castranova V, Fitzpatrick J, Ausman K, Carter J, Karn B, Kreyling W, Lai D, Olin S, Monteiro-Riviere N, Warheit D, Yang H (2005) Principles for characterizing the potential human health effects from exposure to nanomaterials: elements of a screening strategy. Part Fibre Toxicol 2(8):1–35
Oberdörster G, Stone V, Donaldsen K (2007) Toxicology of nanoparticles: a historical perspective. Nanotoxicology 1(1):2–25
RIVM report 320104001/2006 (2006) Cosmetics Fact Sheet to assess the risks for the consumer. Updated version for ConsExpo 4
Rogers RE, Isola DA, Jeng C-J, Levebvre A, Smith LW (2005) Simulated inhalation levels of fragrance materials in a surrogate air freshener formulation. Environ Sci Technol 39(20):7810–7816
Semmler-Behnke M, Kreyling WG, Lipka J, Fertsch S, Wenk A, Takenaka S, Schmid G, Brandau W (2008) Biodistribution of 1.4- and 18-nm gold particles in rats. Small 4(12):2108–2111
Shin JA, Lee EJ, Seo SM, Kim HS, Kang JL, Park EM (2010) Nanosized titanium dioxide enhanced inflammatory responses in the septic brain of mouse. Neuroscience 31(1):99–105
Trudel D, Horowitz L, Wormuth M, Scheringer M, Cousins I, Hungerbühler K (2008) Estimating consumer exposure to PFOS and PFOA. Risk Anal 28(2):251–269
United States Environmental Protection Agency, USEPA (1997) Exposure factors handbook. August 1997
Vernez D, Bruzzi R, Kupferschmidt H, De-Batz A, Droz P, Lazor R (2006) Acute respiratory syndrome after inhalation of waterproofing sprays: a posteriori exposure-response assessment in 102 cases. J Occup Environ Hyg 3(5):250–261
Wallace LA, Emmerich SJ, Howard-Reed C (2004) Source strengths of ultrafine and fine particles due to cooking with a gas stove. Environ Sci Technol 38(8):2304–2311
Willeke K, Baron PA (1993) Aerosol measurement: principles, techniques, and applications. Van Nostrand Reinhold, New York ISBN 0-442-00486-9
Wittmaack K (2007) In search of the most relevant parameter for quantifying lung inflammatory response to nanoparticle exposure: particle number, surface area, or what? Environ Health Perspect 115(2):187–194
Wu J, Liu W, Xue C, Thou S, Lan F, Bi L, Xu H, Yang X, Zeng FD (2009) Toxicity and penetration of TiO2

nanoparticles in hairless mice and porcine skin after subchronic dermal exposure. Toxicol Lett 191(1):1–8

Yamashita M, Takana J, Yamashita M, Hirai H, Suzuki M, Kajigaya H (1997) Mist particle diameters are related to the toxicity of waterproofing sprays: comparison between toxic and non-toxic products. Vet Hum Toxicol 39(2):71–74

Zhu Y, Pudota J, Collins D, Allen D, Clements A, DenBleyker A, Fraser M, Jia Y, McDonald-Buller E, Michel E (2009) Air pollutant concentrations near three Texas roadways, Part I: ultrafine particles. Atmos Environ 43:4513–4522

Nanosized Aerosols from Consumer Sprays: Experimental Analysis and Exposure Modeling

Christiane Lorenz, Harald Hagendorfer, Natalie von Goetz, Ralf Kaegi, Robert Gehrig, Andrea Ulrich, Martin Scheringer, Konrad Hungerbühler

Supplemental Information

Elemental Analysis of TEM images

Product I

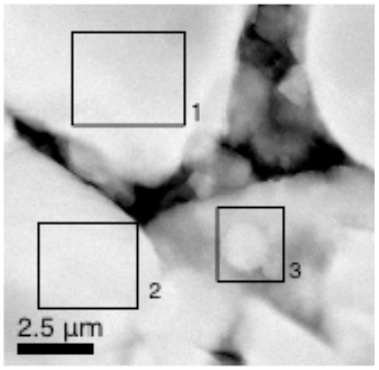

Figure S1A Product I (dispersion) image by STEM. Highlighted are the areas where elemental analysis was performed.

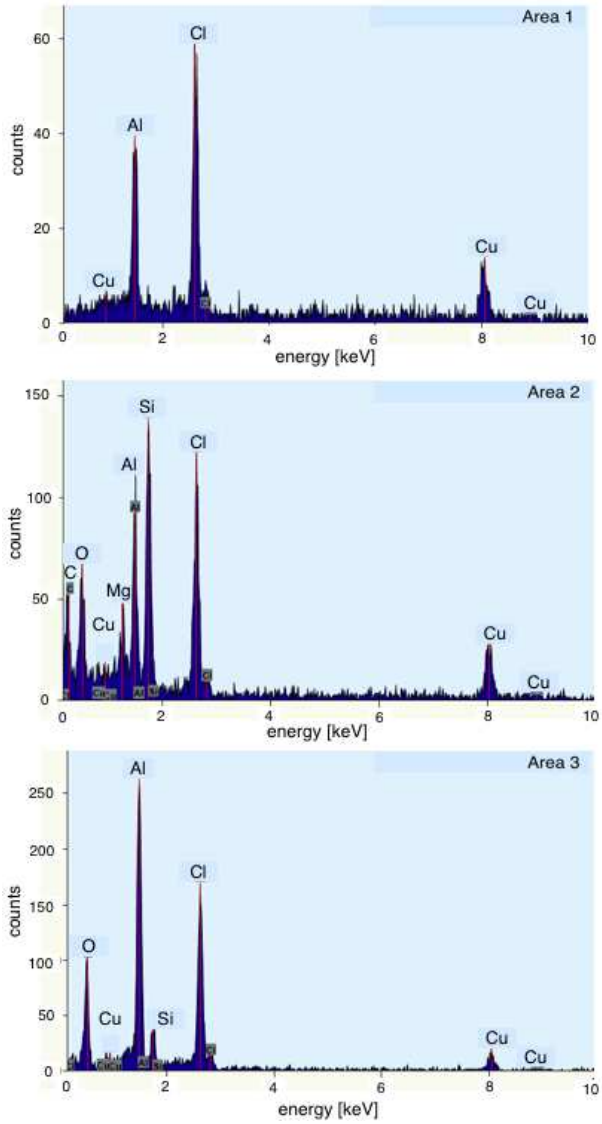

Figure S1B Spectra of product I (dispersion) on the areas highlighted in Figure S1A.

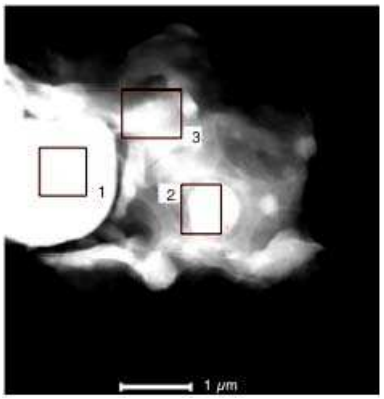

Figure S2A Product I (aerosol) image by STEM. Highlighted are the areas where elemental analysis was performed.

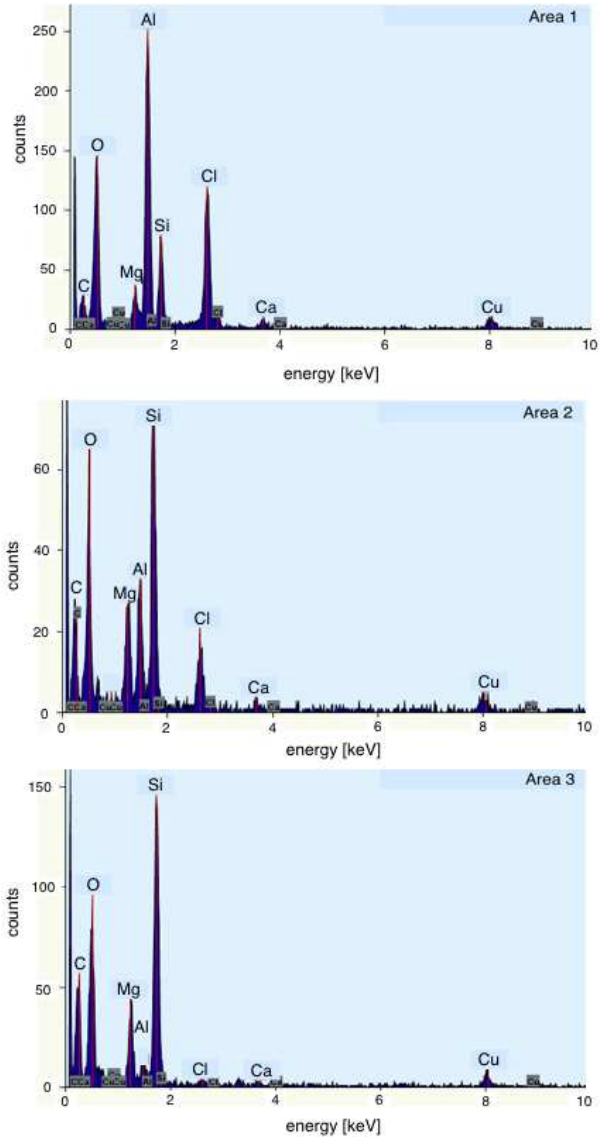

Figure S2B Spectra of product I (aerosol) on the areas highlighted in Figure S2A.

Product II

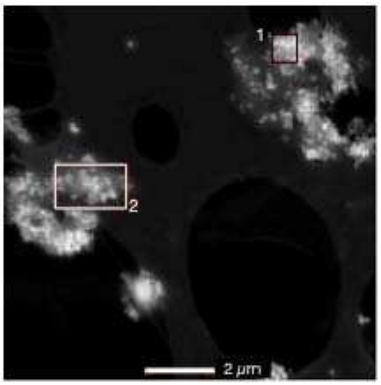

Figure S3A Product II (dispersion) image by STEM. Highlighted are the areas where elemental analysis was performed.

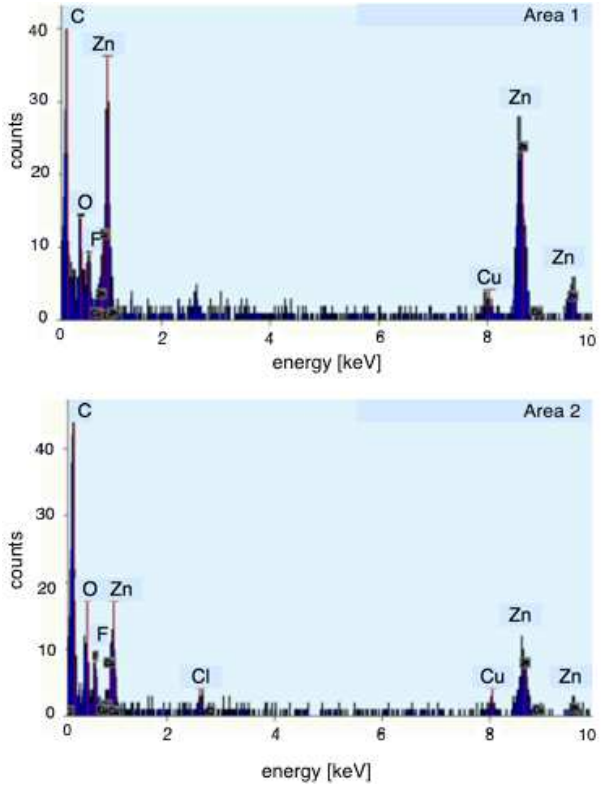

Figure S3B Spectra of product II (dispersion) on the areas highlighted in Figure S3A.

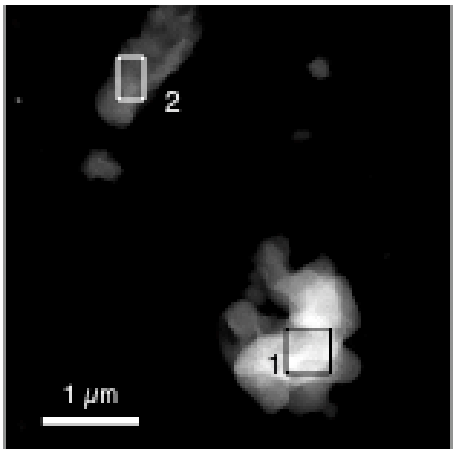

Figure S4A Product II (aerosol) image by STEM. Highlighted are the areas where elemental analysis was performed.

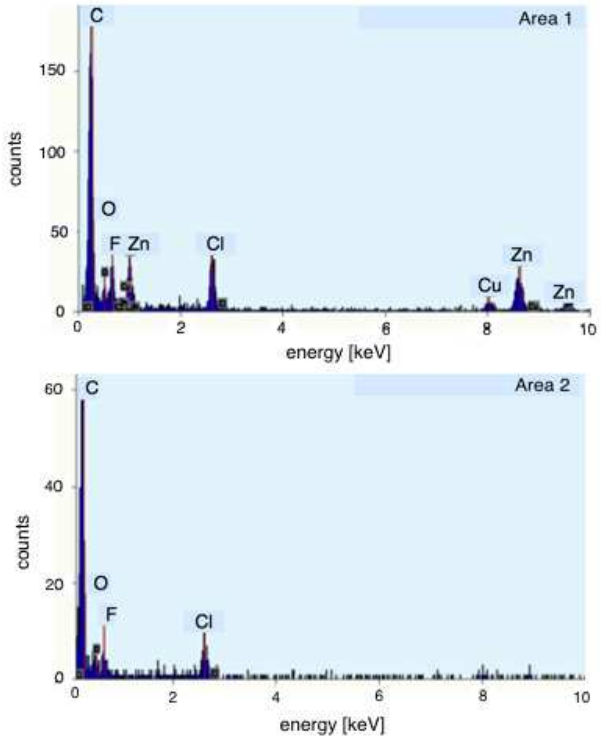

Figure S4B Spectra of product II (aerosol) on the areas highlighted in Figure S4A.

Product III

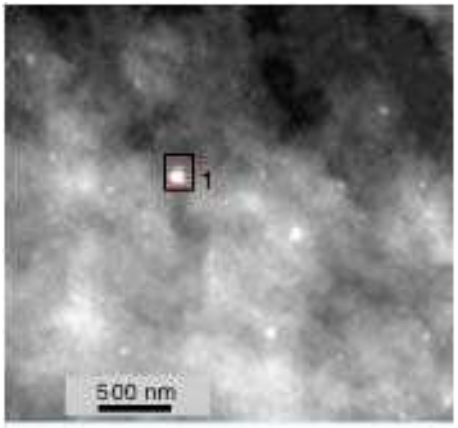

Figure S8A Product III (dispersion) image by STEM. Highlighted are the areas where elemental analysis was performed.

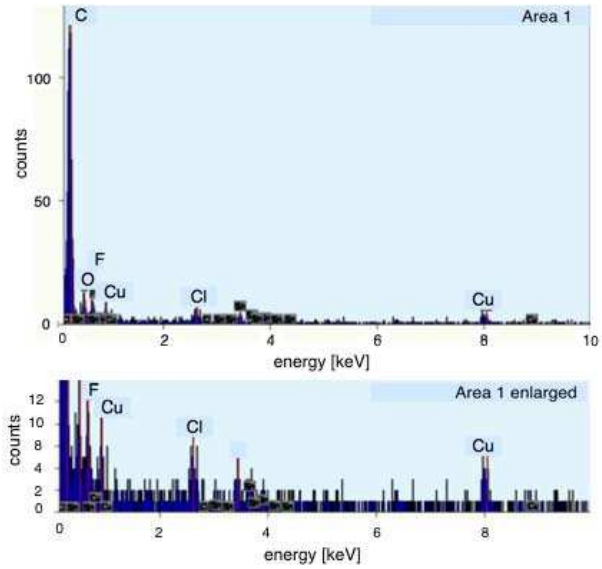

Figure S8B Spectra of product III (dispersion) on the areas highlighted in Figure S8A.

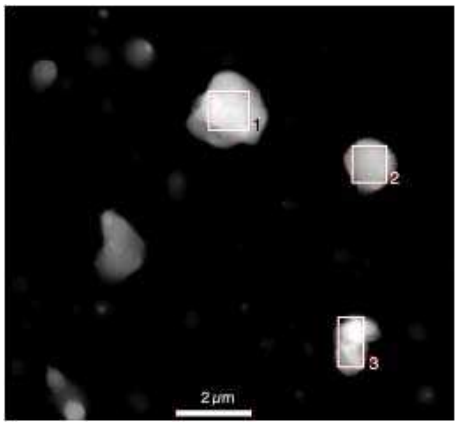

Figure S9A Product III (aerosol) image by STEM. Highlighted are the areas where elemental analysis was performed.

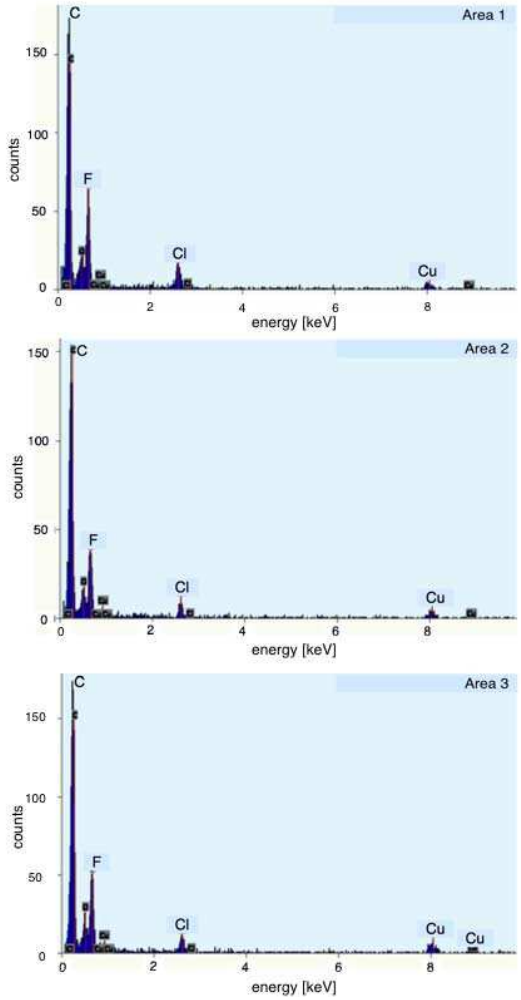

Figure S9B Spectra of product III (aerosol) on the areas highlighted in Figure S9A.

Product IV

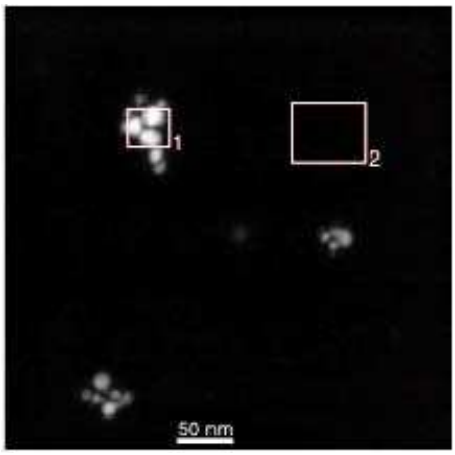

Figure S10A Product IV (dispersion) image by STEM. Highlighted are the areas where elemental analysis was performed.

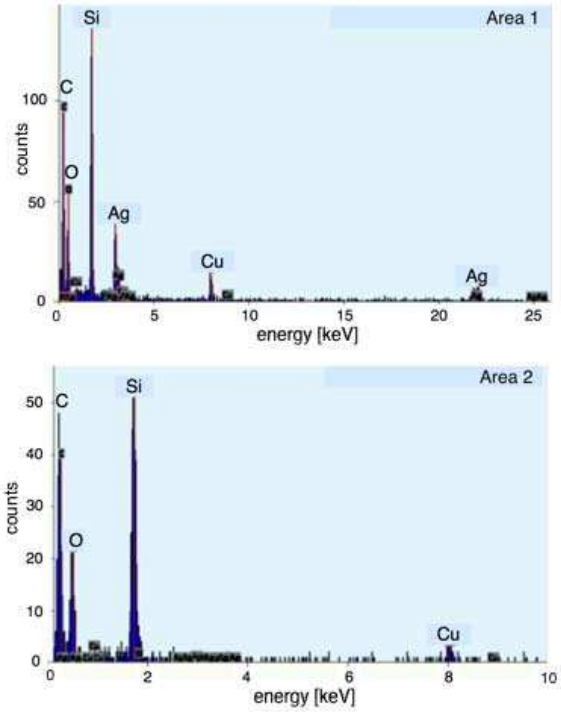

Figure S10B Spectra of product IV (dispersion) on the areas highlighted in Figure S10A.

Particle/droplet size distributions as analyzed by SMPS.

Product I

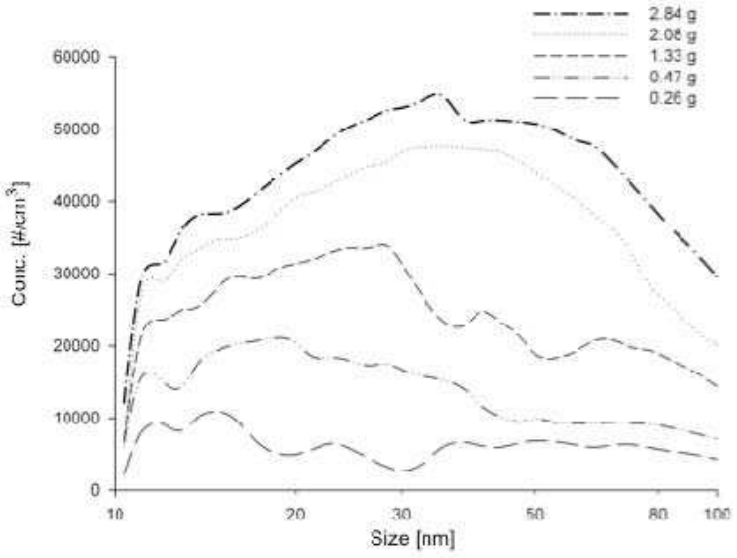

Figure S11 SMPS electropherograms of spray experiments with product I. Different spray masses are indicated. Size distribution taken for modelling: 2.84 g.

Product II

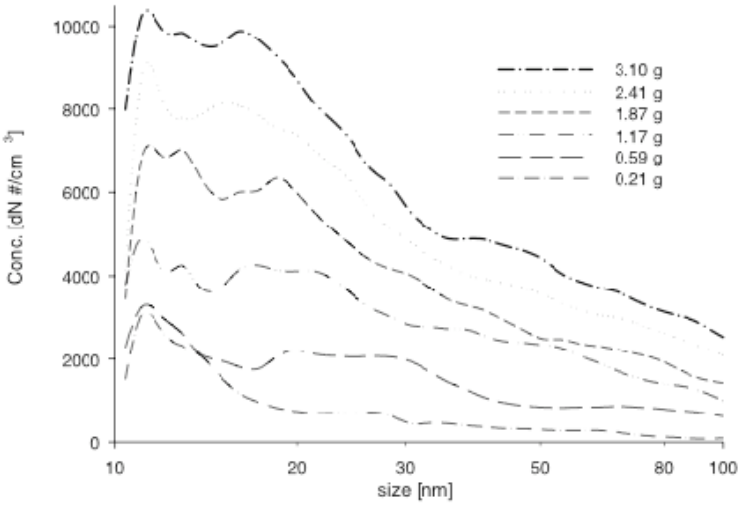

Figure S12 SMPS electropherograms of spray experiments with product II. Different spray masses are indicated. Size distribution taken for modelling: 3.10 g.

Product III

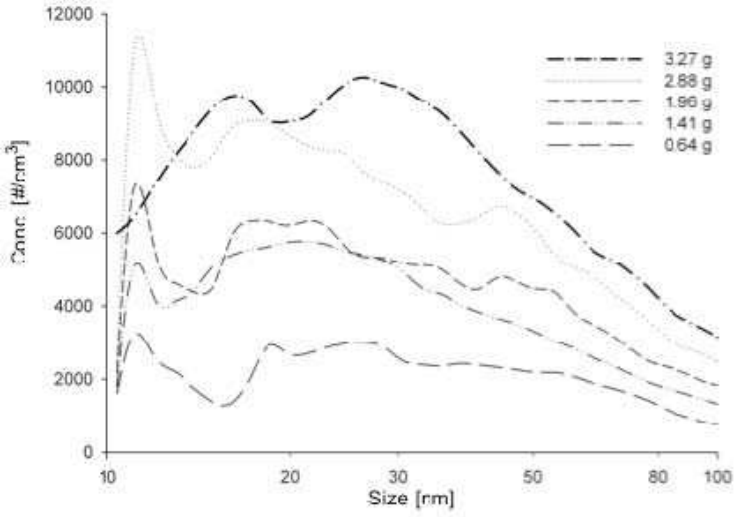

Figure S13 SMPS electropherograms of spray experiments with product III. Different spray masses are indicated. Size distribution taken for modelling: 3.27 g.

Calculations on diffusion losses within tubing of the analytical device

Willeke, K., Baron, P.A., 1993. Aerosol Measurement; Principles, Techniques and Applications. Van Nostrand Reinhold, New York.

$$\eta_{tube,diff} = exp(-\pi dLV_{diff} / Q)$$

$$Sh = 3.66 + \frac{0.0668\,(d/L)\,Re_f\,Sc}{1 + 0.04[(d/L)\,Re_f\,Sc]^{2/3}}$$

d	Tube diameter: 0.5 cm
L	Tube length: 50 cm
V_{diff}	Deposition velocity for particle diffusion loss to the wall
Q	volumetric air flow Air flow rate: cm^3/s
Re_f	Reynolds number
Sc	Schmidt number
Sh	Sherwood number [-]

Temperature: 295 K
Pressure: 96 kPa

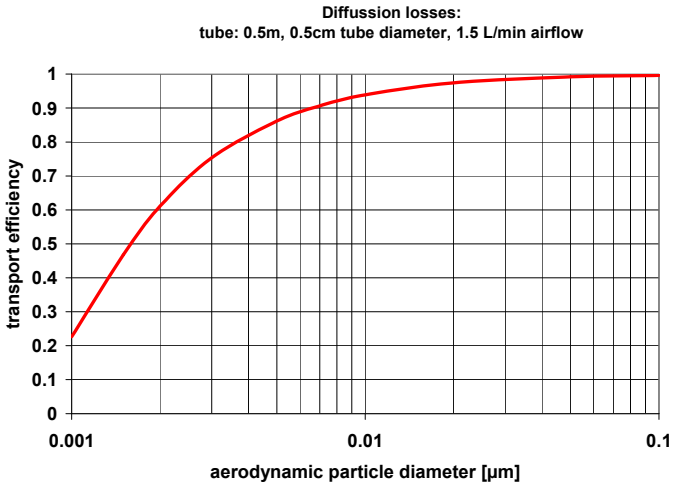

Figure S13 Estimated transport efficiency of engineered nanoparticles through the measurement device illustrated in Figure 1 (main text).

SMPS size fractions:

Table S1 List of SMPS size fractions collected during spray experiments.

j	size fraction as labelled by SMPS (average of size range) [nm]	size fraction [nm]			time within SMPS cycle [s]
		minimum	maximum	range	
1	10.4	10.00	10.75	0.75	8
2	11.1	10.75	11.55	0.80	11
3	12	11.55	12.45	0.90	14
4	12.9	12.45	13.35	0.90	17
5	13.8	13.35	14.35	1.00	20
6	14.9	14.35	15.45	1.10	23
7	16	15.45	16.60	1.15	26
8	17.2	16.60	17.80	1.20	29
9	18.4	17.80	19.10	1.30	32
10	19.8	19.10	20.55	1.45	35
11	21.3	20.55	22.10	1.55	38
12	22.9	22.10	23.75	1.65	41
13	24.6	23.75	25.50	1.75	44
14	26.4	25.50	27.40	1.90	47
15	28.4	27.40	29.45	2.05	50
16	30.5	29.45	31.65	2.20	53
17	32.8	31.65	34.00	2.35	56
18	35.2	34.00	36.55	2.55	59
19	37.9	36.55	39.30	2.75	62
20	40.7	39.30	42.20	2.90	65
21	43.7	42.20	45.35	3.15	68
22	47	45.35	48.75	3.40	71
23	50.5	48.75	52.35	3.60	74
24	54.2	52.35	56.25	3.90	77
25	58.3	56.25	60.45	4.20	80
26	62.6	60.45	64.95	4.50	83
27	67.3	64.95	69.80	4.85	86
28	72.3	69.80	75.00	5.20	89
29	77.7	75.00	80.60	5.60	92
30	83.5	80.60	86.65	6.05	95
31	89.8	86.65	93.15	6.50	98
32	96.5	93.15	100.10	6.95	101

Extrapolation of aerosol particle and droplet concentrations

Table S2 Equations of linear fits illustrated in Figure 3 in the main text.

Product	m [#/cm^3]	n [#/g cm^3]	a_{spray} [g]	C_{inhal} [#/cm^3]
I, antiperspirant	1.66 x 10^5	4.55 x 10^5	4.00	1.98 x 10^6
II, shoe spray (boot women)	1.43 x 10^4	6.08 x 10^4	12.65	7.84 x 10^5
II, shoe spray (boot men)	1.43 x 10^4	6.08 x 10^4	18.48	1.14 x 10^6
III, shoe spray (boot women)	1.75 x 10^4	6.81 x 10^4	12.65	8.79 x 10^5
III, shoe spray (boot men)	1.75 x 10^4	6.81 x 10^4	18.48	1.28 x 10^6